



Effect of defatted walnut powder extract on pigment gallstones and its metabolism *in vitro*

Shi-nuo FANG¹, Xia-jing XU¹, Jing MA¹, Qing-zhu ZHANG¹, Dong-mei WANG², Ying-ni PAN¹, Shu-meng REN^{1*},
Xiao-qiu LIU^{1*} 

Abstract

Gallstones disease is classified as cholesterol, pigment and mixed gallstones. Pigment gallstones is a common disease, and some patients experienced complications such as biliary pain and cholecystitis. Defatted walnut powder extract (DWPE) is extracted from the main by-product after oil extraction of the functional food walnut and can treat cholesterol gallstones. However, the effect of DWPE on pigment gallstones has not been reported. Thus, this paper aimed at exploring the potential mechanism of alleviating pigment gallstones and the metabolism of DWPE *in vitro* by UPLC-Q-Exactive Orbitrap MS to elucidate potential pharmacodynamic substances. It was found that DWPE significantly reduced the incidence of gallstones, the contents of unconjugated bilirubin and calcium, the inflammation of gallbladder tissue, the edema and congestion of gallbladder tissue, and the infiltration of inflammatory cells. In metabolism, a total of 35 metabolites of DWPE, including its main compounds ellagic acid and glansreginin A, were characterized in the intestine with various metabolic reactions. Presumably, the small molecular compounds generated after the metabolism by intestinal bacteria may be the pharmacodynamic substances of DWPE on pigment gallstones. This study revealed the effect of DWPE in treating pigment gallstones and their metabolism *in vitro*.

Keywords: defatted walnut powder extract; pigment gallstones; metabolic analysis *in vitro*; intestinal bacteria; UPLC-Q-Exactive Orbitrap MS; glansreginin A.

Practical Application: Protection of pigment gallstones disease by defatted walnut powder extract and its metabolism *in vitro*.

1 Introduction

Gallstones disease is a common disease caused by biliary component abnormality and biliary movement dysfunction (Swarne et al., 2021), which can be divided into cholesterol gallstones, pigment gallstones (PGS) and mixed gallstones (Lu et al., 2021). Gallstones disease is a frequent condition all over the world with the incidence of 10%-20% in China, and there are millions of patients with PGS in China (Yao et al., 2019). Although it can be treated by surgery, severe syndromes such as dyspepsia and biliary obstruction will occur after surgery (Beckingham, 2020). At present, the main problems of medication therapy for PGS are the numerous side effects and high recurrence rate. Traditional Chinese medicine has the benefit of limiting toxic side effects while still producing curative effects (Wei et al., 2023). Thus, the intention of using traditional Chinese medicine for the treatment of PGS is increasing.

As a popular nut, walnut kernel has great popularity as functional food in the international market with high nutritional value and deliciousness, which is used as the homology of medicine and food in China (Cheng et al., 2022; Xu et al., 2022a; Xu et al., 2022b). Defatted walnut powder is the residue of walnut oil extracted from walnut kernel (Qu et al., 2021), which retains the main nutrients of walnut except fat. Pharmacological studies have shown that the phenolic compounds in defatted walnut powder extract (DWPE) exhibited various biological activities, including lowering lipids (Ruiz-Caro et al., 2022), anti-oxidation (Chen et al., 2021), hypoglycemic (Duan et al.,

2020) and treating hypercholesterolemia (Ashraf et al., 2021; Gao et al., 2022). According to our previous study, DWPE effectively reduced the formation of cholesterol gallstones by participating in the protective effect against liver injury and regulating liver metabolism (Ren et al., 2018). There are some similarities between cholesterol gallstones and PGS. Cholesterol gallstones is composed of a higher percentage of cholesterol and less calcium salts of bilirubin and phosphates. PGS is composed of a higher percentage of bilirubin calcium and less than 30% cholesterol (Swarne et al., 2021). The pathophysiology of cholesterol gallstones disease involved biliary cholesterol secretion imbalances, inflammatory reactions in the epithelium of the gallbladder, mucin production and gallbladder motility disturbances. Differently, PGS is caused by abnormal bilirubin metabolism and pigmentation as a result of large amounts of bilirubin precipitation (Wang et al., 2020). However, it is not clear whether DWPE has the ability to treat PGS. Therefore, the effect of DWPE on the treatment of PGS was studied.

To further explore the substance basis of DWPE in the treatment of PGS, the study of the metabolism of DWPE was necessary. As we known, drug metabolism in the body is a complex progress. DWPE produced extensive metabolic reactions in rats and the absorbed compounds *in vivo* were mainly the metabolites of glansreginin A (Gla A), gallic acid (GA), and ellagic acid (EA), which were the effective components of DWPE *in vivo* (Bidanchi et al., 2022; Haramiishi et al., 2020; Tošović & Bren,

Received 02 Oct., 2022

Accepted 29 Nov., 2022

¹School of Traditional Chinese Medicine, Shenyang Pharmaceutical University, Shenyang, Liaoning, China

²School of Pharmacy, Shenyang Pharmaceutical University, Shenyang, Liaoning, China

*Corresponding author: liuxiaoqiu3388@126.com; renshumeng0718@163.com

2020). Previous studies only studied the metabolism of DWPE *in vivo*, but the metabolic site of DWPE *in vivo* is still unclear. After oral administration, most components were biotransformed to create numerous metabolites under the influence of various factors, such as the pH levels of gastric and intestinal juice, pepsin, trypsin and intestinal bacteria (Wang et al., 2019). Therefore, it is necessary to further study the metabolism of DWPE *in vitro*.

In this study, the anti-PGS effect of DWPE in guinea pigs was studied by assessing histopathological changes and bile biochemical indices. Meanwhile, the metabolic stability and metabolites of DWPE, EA and Gla A *in vitro* were analyzed by UPLC-Q-Exactive Orbitrap MS to further reveal the metabolic mechanism and pharmacodynamic substances of DWPE.

2 Material and methods

2.1 Chemicals, reagents and extract preparation

Walnut kernel was collected from Xinjiang province, China, and authenticated as the seed of *Juglans regia* L., by Dr. Yingni Pan from Shenyang Pharmaceutical University. They were immersed in a 5-fold volume of petroleum ether for 1 h and sonicated three times for 30 min each time. After having been filtered, the supernatant was evaporated to remove petroleum ether. The residues were collected and refluxed thrice with a 10-fold volume of 60% ethanol for 1.5 h, and then the filtrate was evaporated, concentrated, and exsiccated to prepare DWPE.

GA and EA were obtained from Chengdu Pufei De Biotech Co., Ltd (> 98%). Gla A was prepared in our laboratory (> 98%). Ursodeoxycholic acid tablets (UDCA, no. 41170402) were obtained from Shanghai Xinyi Pharmaceutical Factory. Lincomycin (no. 1704349) was obtained from Sinopharm Group Rongsheng Pharmaceutical Co. Ltd. UPLC-grade acetonitrile, formic acid and purified water were obtained from Sigma Aldrich (Steinheim, Germany), Damao Chemical Reagent Factory (Tianjin, China) and Wahaha group Co. Ltd (Hangzhou, China), respectively.

2.2 Animals

Sprague-Dawley rats (220 ± 20 g) and Hartley guinea pigs (300 g ± 20 g) were purchased from the Animal Experiment Center of Shenyang Pharmaceutical University (Liaoning, China). Animals were housed under a constant environmental condition (temperature: 25 ± 1 °C) and entrained to a 12 h light-dark cycle with ad libitum feeding. All the animal experiments were performed in accordance with the Guide for the Care and Use of Laboratory Animals, and followed the Shenyang Pharmaceutical University Animal Experimentation Guidelines.

2.3 Animal experiments

The lithogenic diet contained 3% sucrose, 2% casein, 2% lard, 2% microcrystalline cellulose, 0.1% cholesterol, 0.04% sodium cholate, and the basal diet contained 11% water, 17% crude protein, 3% crude fat, 9% crude ash and 15% crude fiber.

Thirty guinea pigs were randomly divided into five groups: control group, model group, DWPE low-dose (L-DWPE) group, DWPE high-dose (H-DWPE) group and ursodeoxycholic acid (UDCA) group. Cystic bile and gallbladder tissue were collected on the last day. Part of the gallbladder was placed in 10% neutral formalin solution for histopathological examination, and the other part was stored at -40 °C with cystic bile (Figure 1).

2.4 Pathological examination

Gallstones were detected for the presence of cholesterol crystals using light microscopy and polarizing light microscopy. The characteristic of gallstones was analyzed by infrared spectroscopy after being ground and compressed into potassium bromide disks. Sections of gallbladder were fixed in 10% formalin for 24 h and embedded in paraffin. Then, the sections were stained with hematoxylin and eosin, and examined by light microscopy.

2.5 Measurement of serum calcium and bilirubin

Calcium in the serum was examined using calcium assay kit from Nanjing Jian cheng Bioengineering Institute (#C004-2-1), Total bilirubin (TBIL) kit (#C019-1-1) and Direct bilirubin (DBIL) kit (#C019-2-1) according to the manufacturer's instruction. The difference between TBIL and DBIL measurements was the concentration of unconjugated bilirubin (UCB) (Dhungana et al., 2017).

2.6 UPLC-Q-Exactive Orbitrap MS data acquisition of DWPE

Chromatographic separation was performed on a Waters ACQUITY UPLC coupled with a LTQ-Orbitrap XL mass spectrometer system (Thermo Scientific, Bremen, Germany) using an ACQUITY UPLC BEH C18 column (2.1 × 100 mm, 1.7 μm) by gradient elution using acetonitrile (A) and 0.1% formic acid in water (B). The flow rate was 0.3 mL/min and the detector wavelength was 254 nm. The gradient program was as follows: 0-2.5 min, 5-15% (A); 2.5-5 min, 15-25% (A); 5-8 min, 25-28% (A); 8-9 min, 28-50% (A). The LTQ-Orbitrap XL mass spectrometer system coupled with a heated electrospray ionization (HESI) source was operated in negative ion mode. The MS parameters were as follows: capillary voltage,

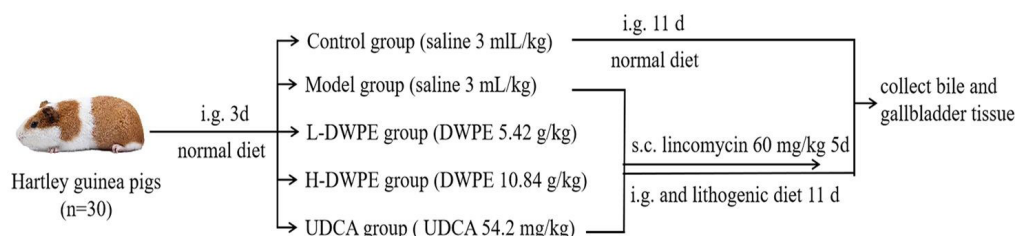


Figure 1. Experimental design for studying the treatment of PGS in guinea pigs by DWPE.

3.5 kV; source temperature, 300 °C; Aux gas heater temperature, 320 °C; sheath gas and aux gas flow rate, 40 and 10 arb, respectively. The samples were analyzed using Full MS/dd-MS2 scan and the resolution was set to 70000. The normalized collision energy was set at alternative voltages of 20, 40 and 60 eV. Centroid mode data was collected over the range of 80-1200 m/z. The mass data were analyzed by Xcalibur 2.1 and Compound Discoverer 3.0 software. DWPE, GA, EA and Gla A were injected into the UPLC system for analysis with the final concentrations at 2 mg/mL, 0.030 mg/mL, 0.050 mg/mL and 0.052 mg/mL, respectively.

2.7 Incubations of DWPE in simulated gastrointestinal digestion

Simulated gastric and intestinal juice was prepared by the 2020 edition of Chinese pharmacopoeia (Chinese Pharmacopoeia Commission, 2020). DWPE, EA and Gla A were added into gastric and intestinal juice incubation mixture with the final concentrations at 6 mg/mL, 1 mM and 1 mM, respectively. The incubations were placed in the incubator at 37 °C for 45 min. The incubations were sampled at 0, 1, 2, 3, 4, 5 and 6 h and were added into the precooled solution of methanol containing 1% formic acid in the ratio of 1:2 (v/v). The samples were immediately vortex mixed for 30 s, followed by centrifuging at 12,000 rpm for 10 min. After filtration using microporous filter membrane of 0.22 µm, the sample was analyzed by UPLC.

2.8 Incubations of DWPE in rat intestinal bacteria

The general anaerobic medium content (g/L): 15.0 g peptone, 13.5 g digestibility serum powder, 10.0 g tryptone, 5.0 g yeast extract, 2.5 g KH₂PO₄, 0.3 g soya starch, 0.3 g L-cysteine hydrochloride and 0.15 g sodium thioglycolate. Anaerobic broth powder (6.0 g) was accurately weighted and dissolved in distilled water, and then adjusted to pH 7.2 before adjusting to a total volume of 100 mL. The obtained anaerobic medium was autoclaved at 121 °C for 20 min.

Preparation of intestinal bacterial juice: Fresh feces (1 g) were weighed and homogenized in 4 mL physiological saline solution immediately. The homogenate was removed into 10 mL centrifuge tube and centrifuged for 10 min at 3000 rpm. The supernatant was obtained as intestinal bacterial mixture.

DWPE, EA and Gla A were added into bacterial solution with the final concentrations at 2.14 mg/mL, 0.14 mg/mL and 0.11 mg/mL, respectively. The blank group without samples and the control group with sterilized intestinal bacteria mixture vortex mixed and incubate at 37 °C for 48 h. The incubations were sampled at 0, 2, 4, 6, 8, 12, 24, 36 and 48 h, and added precooled solution of methanol containing 1% formic acid. The sample was immediately vortex mixed for 60 s, followed by centrifuging at 12,000 rpm for 10 min. After filtration using microporous filter membrane of 0.22 µm, the sample was analyzed by UPLC-Q-Exactive Orbitrap MS.

2.9 Statistical analysis

Statistical analysis was performed by GraphPad Prism 8.0 and the data were shown as mean ± SD. All data analysis was examined by ANOVA by Tukey's Multiple Comparison Test.

3 Results

3.1 Analysis of pathological examination

The bile was pale yellow and clear, with no formation of gallstone in the control, H-DWPE and UCDA groups. In the model and L-DWPE groups, stones were observed by eyes (Figure 2A). The results of light microscope and polarizing microscope of PGS were shown in Figure 2B. The relative areas of gallstones were shown in Figure 2C. Model group showed several amorphous granular stones. The core was mostly irregular structure, and there was no obvious crystalline material around the core. Compared with the control group, the gallstones area in the model group was significantly increased. The gallstones were still observed in the L-DWPE group, but the area was smaller than the model group. UDCA and H-DWPE groups fully blocked the lithogenic effects with few gallstones, which were significantly different from the model group. Thus, we inferred that DWPE inhibited the formation of gallstones. The gallstones defined as bilirubin calcium-pyrophosphate pigment gallstones, and had absorption peaks at 3424.2 cm⁻¹, 1610.1 m⁻¹, 1440.3 cm⁻¹, 1011.4 cm⁻¹ (Figure 2D).

Severe interstitial edema, vascular dilation, hyperemia and infiltration of inflammatory cells were brought on by the lithogenic diet and lincomycin injection in the model group. Villi atrophy and slight interstitial edema appeared in the L-DWPE group. Gallbladder lesions in the H-DWPE and UDCA groups were significantly improved, with less inflammation, no tissue hyperemia and abnormalities in the villi. (Figure 2E).

3.2 Analysis of Ca²⁺, TBIL and UCB

Compared with the control group, the contents of TBIL, UCB and Ca²⁺ in the model group were significantly increasing. Compared with the model group, H-DWPE group, L-DWPE group and UDCA group were significantly decreased in TBIL and UCB, respectively (Figure 3A-3B). The contents of Ca²⁺ in the H-DWPE group, L-DWPE group and UDCA group were lower than the model group, but the differences were not significant (Figure 3C).

3.3 UPLC analysis of DWPE

The result showed that the peak 1, peak 3 and peak 4 were attributed to be GA, EA and Gla A, respectively, according to compared with compounds standards (Figure 4). The peak 2 was ellagic acid 4-O-xyloside (EA-Xyl), according to the relative content and retention time (Ren et al., 2022). According to the chromatograms, EA-Xyl, EA and Gla A are the main components, so the following *in vitro* metabolism mainly focuses on these three compounds.

3.4 Stability studies of DWPE in simulated gastric and intestinal juice

The stability results of DWPE, EA and Gla A incubated with simulated gastric and intestinal juice for 6 h were shown in Figure 5A-5B. Since EA-Xyl, EA and Gla A were relatively high in DWPE, they were used as the representative components of DWPE. EA-Xyl, EA and Gla A in DWPE, EA and Gla A were

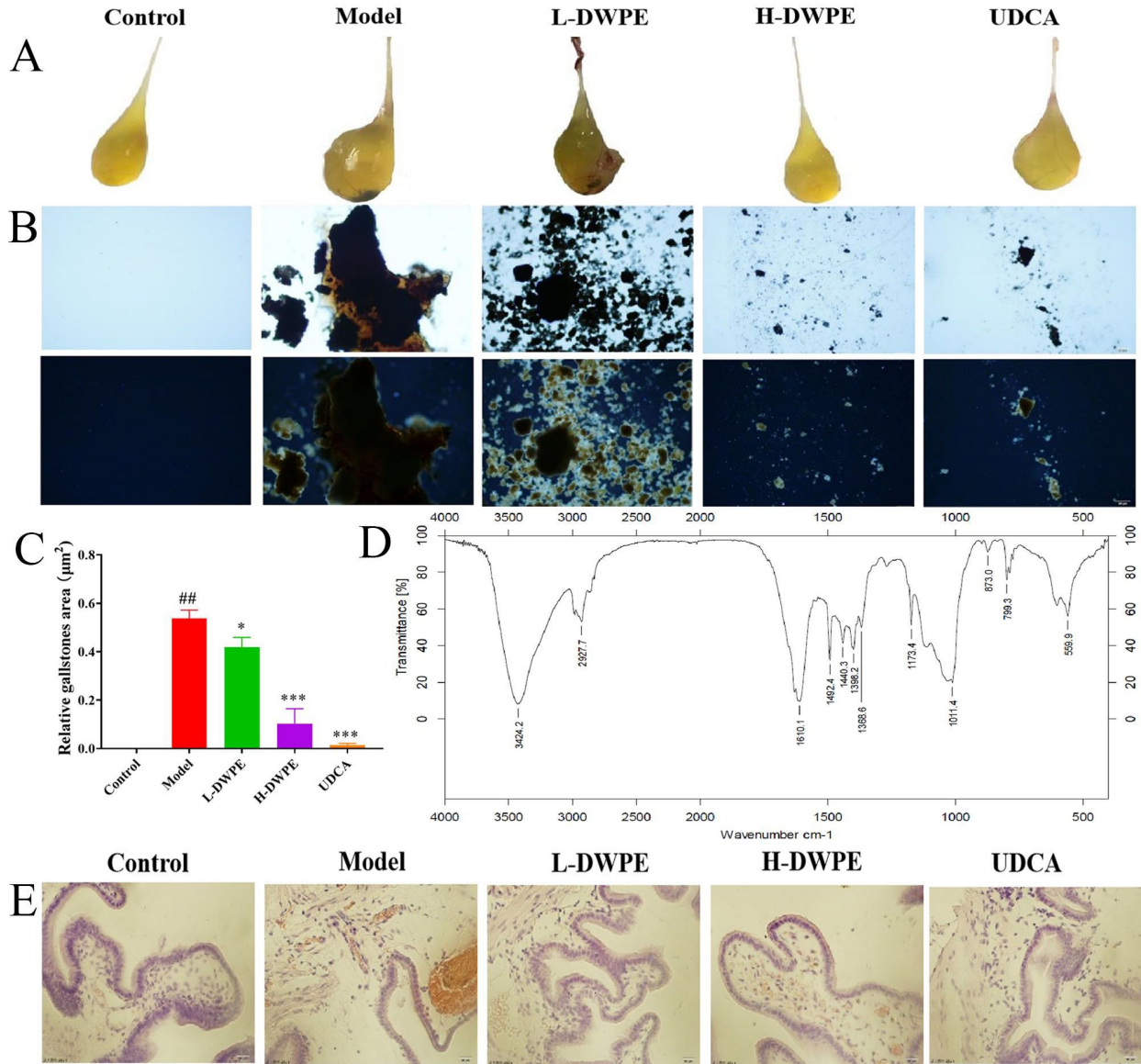


Figure 2. Effect of DWPE on gallstones formation in different groups. (A) Gallbladder stone formation; (B) Images of bile sludge visualized with light microscopy and polarizing light microscopy (200 \times); (C) The relative gallstones areas; (D) Infrared spectrum; (E) Histopathological observation of gallbladder (200 \times). Compared with control group: ## $p < 0.01$. Compared with model group: * $p < 0.05$, *** $p < 0.001$.

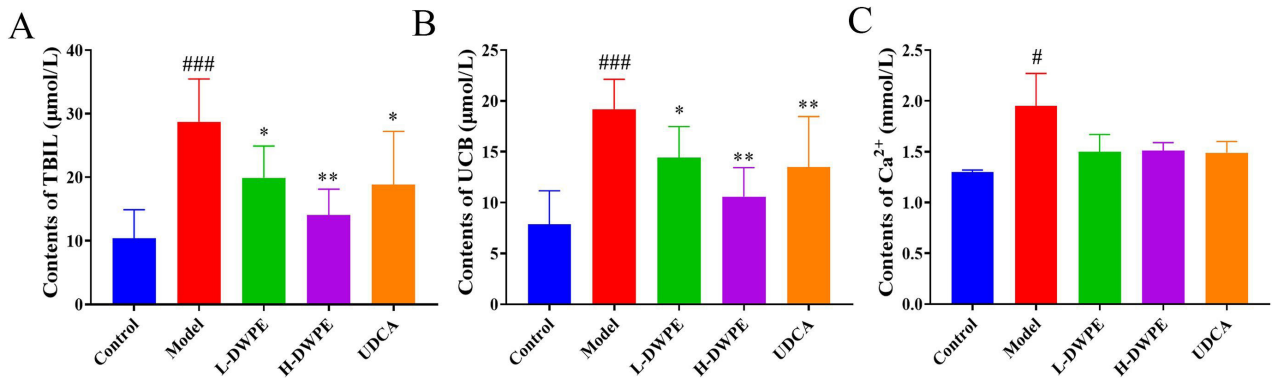


Figure 3. Contents of TBIL (A), UCB (B) and Ca^{2+} (C) in the bile. Compared with control group: * $p < 0.05$, ### $p < 0.001$. Compared with model group: # $p < 0.05$, ** $p < 0.01$.

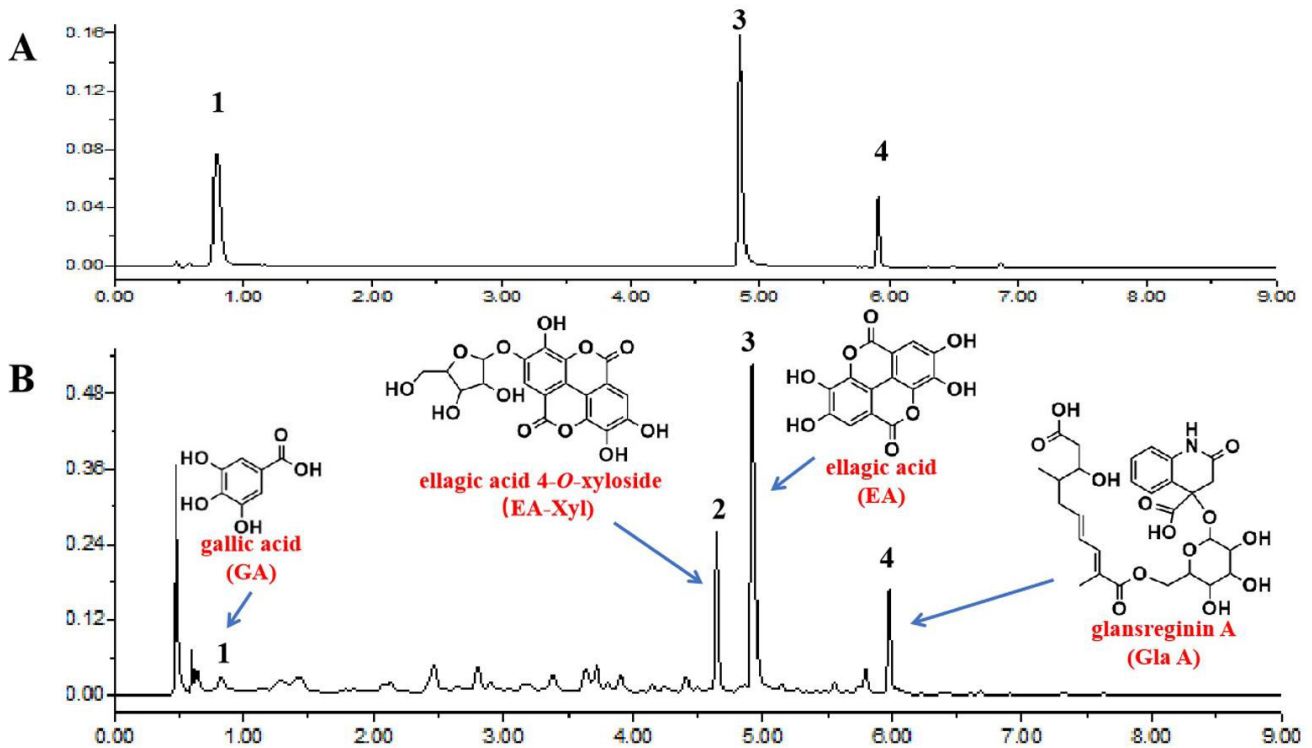


Figure 4. Chromatograms of compounds standards (A) and DWPE (B). 1: GA; 2: EA-Xyl; 3: EA; 4: Gla A.

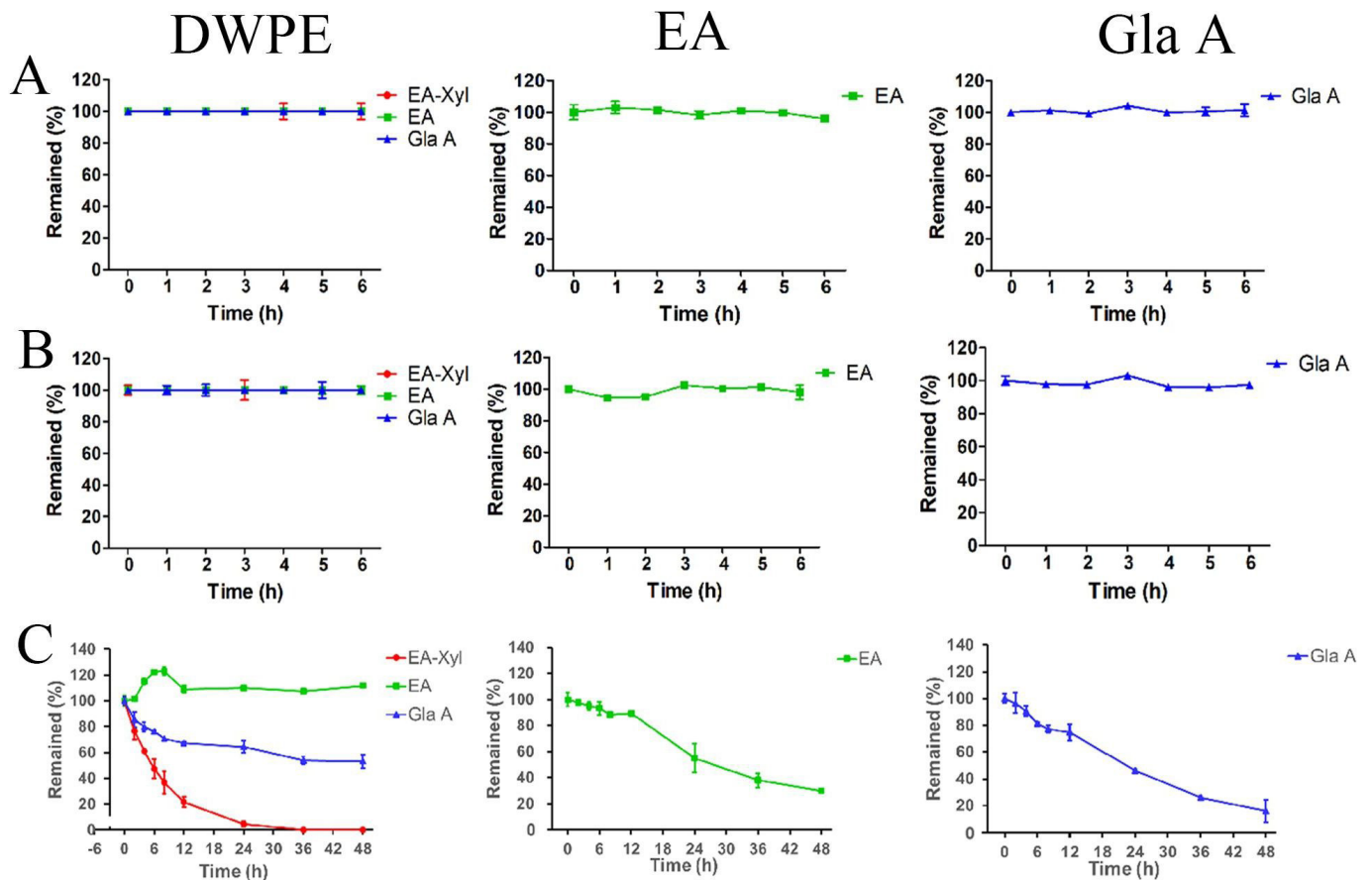


Figure 5. Stability results of DWPE, EA and Gla A in simulated gastric juice (A), simulated intestinal juice (B) and intestinal bacteria (C).

found stable in simulated gastric and intestinal juice, in which the compounds did not change significantly according to the peak area during 6 h of incubation, and the RSD was all less than 3.0%. There was no new chromatographic peak generated. Therefore, it was indicated that DWPE, EA and Gla A were relatively stable in simulated gastric and intestinal juice for 6 h.

3.5 Stability studies of DWPE in intestinal bacteria

The concentration of EA in DWPE was increased in 6 h, decreased in the next 6 h, and then stabilized after 12 h. The concentrations of EA-Xyl and Gla A in DWPE were decreased rapidly within 12 h, and dropped to 5% and 50% after 24 h, respectively. The results suggested that the increase of EA content within 6 h may be caused by the deglycosylation of EA-Xyl to EA. The concentrations of EA and Gla A monomers were respectively decreased to 30% and 16% in 48 h (Figure 5C).

3.6 Analysis of metabolites in intestinal bacteria

The metabolites of DWPE, EA and Gla A cultured with rat intestinal bacteria for 48 h under anaerobic conditions were analyzed by UPLC-Q-Exactive Orbitrap MS (Figure 6). Totally of 35 prototype components and metabolites were detected. The result indicated that the proposed metabolic pathways were phase I

metabolic reactions including dehydroxylation, hydroxylation, hydrolysis, hydration and hydrogenation, and phase II metabolic reaction of methylation. Detailed mass information of DWPE, EA, Gla A and their metabolites in intestinal bacteria were shown in Table S1. The metabolic pathways were shown in Figure 7.

Analysis of the metabolites of DWPE in intestinal bacteria

A total of 30 metabolites of DWPE in intestinal bacteria were identified, including **M1-M5**, **M7-M13**, **M15-M18**, **M20**, **M22-M33** and **M35**. The result indicated that the possible metabolic pathways were methylation, hydrolyzation, hydration, dehydration, reduction and desaturation.

M20 and **M29** were identified as EA and Gla A, respectively, by comparing with the authentic standard for their retention time, molecular ion peaks and fragment ions. According to previous literatures, the fragment ions at m/z 403.16006, 241.10811, 188.03487 and 144.04514 were characteristic fragment ions of Gla A, and the fragment ions at m/z 283.99585 and 257.00977 were characteristic fragment ions of EA (Ren et al., 2022). **M11** and **M24** were attributed to be urolithin M5 and glansreginic acid 8-O- β -D-glucoside, respectively. Urolithin M5 was identified as the hydrolyzation product of EA. **M12** was considered to be glansreginic acid 8-O- β -D-glucoside+H₂O+2H, with [M-H]⁻ ion

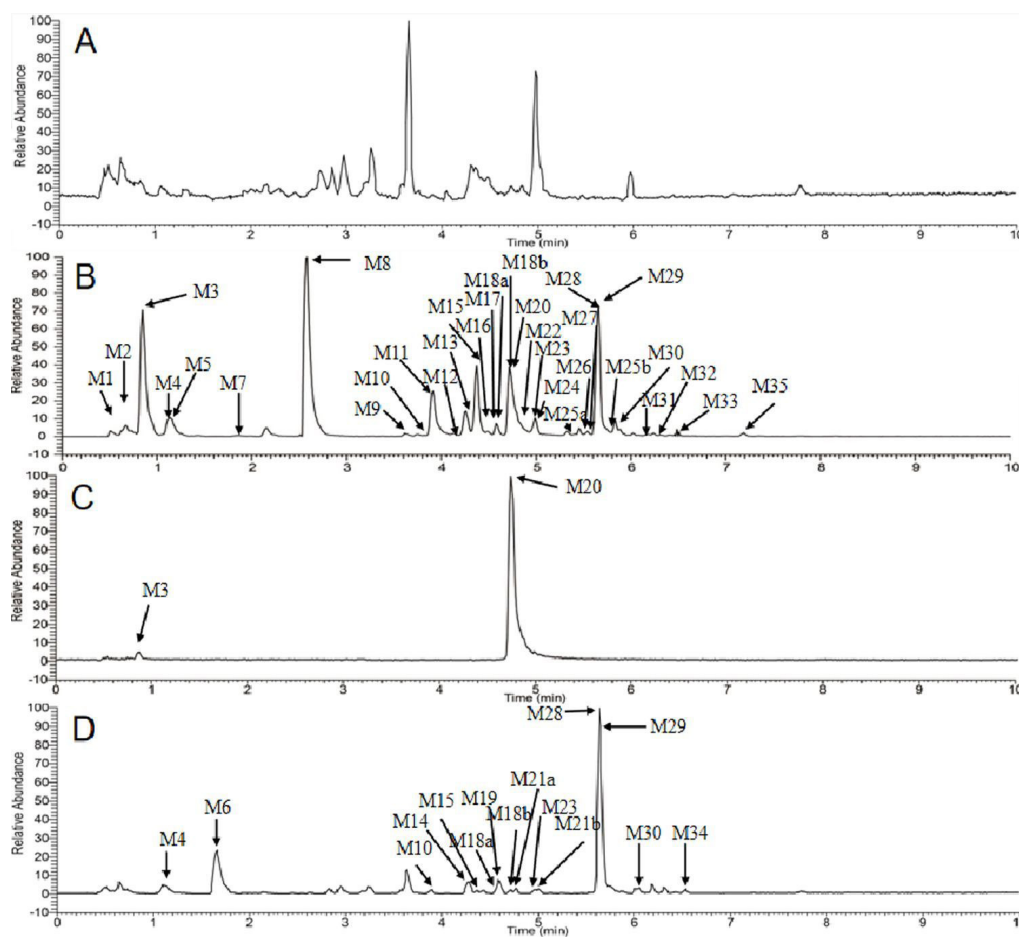


Figure 6. The extracted ion chromatograms of blank intestinal bacteria (A), DWPE metabolites (B), EA metabolites (C) and Gla A metabolites (D) in intestinal bacteria in the negative ion mode.

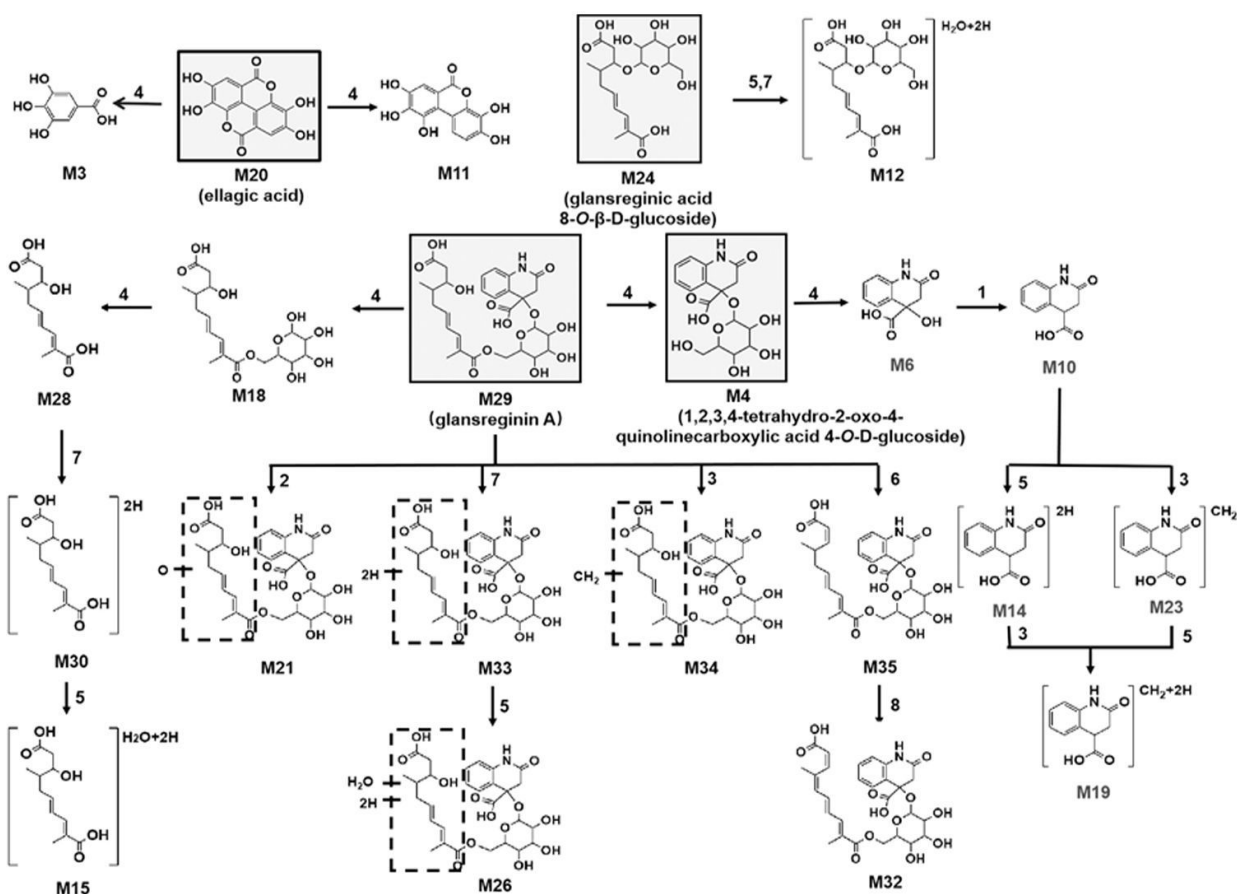


Figure 7. The proposed metabolic pathways of metabolites of DWPE, EA and Gla A in rat intestinal bacteria. 1: dihydroxylation; 2: hydroxylation; 3: methylation; 4: hydrolyzation; 5: hydration; 6: dehydration; 7: hydrogenation; 8: dehydrogenation.

at m/z 423.187842, and fragmentation ion at m/z 243.12373, which was 20 Da (H_2O+2H) higher than that of **M24**.

Gla A was hydrolyzed into 2 metabolites including **M18** (glansreginic acid- O - β -D-glucopyranosylester) and **M4** (1,2,3,4-tetrahydro-2-oxo-4-quinolinecarboxylic acid 4- O -D-glucoside) (Ren et al., 2022). **M28** was considered to be glansreginic acid with characteristic ion at m/z 197.11841 and deprotonated molecular ion $[M-H]^-$ ion at m/z 241.10849, which were 162 Da ($-Glc$) lower than **M18**. **M30** showed $[M-H]^-$ ion at m/z 243.12410 and a fragment ion at m/z 199.13412, which were 2 Da ($2H$) higher than glansreginic acid. Hence, **M30** was inferred as glansreginic acid+ $2H$. **M15** exhibited $[M-H]^-$ ion at m/z 261.13455, which was 20 Da higher than **M28**. The fragmentation ions at m/z 201.11327 and 199.13419 were found, which were 20Da and 18Da higher than the fragment ion at m/z 181.08702 of **M28**. So **M15** was identified as glansreginic acid+ H_2O+2H . **M10** had a characteristic ion at m/z 144.04549 and a deprotonated molecular ion $[M-H]^-$ at m/z 190.05104, which were 178 Da ($-Glc-O$) lower than **M4**. Thus, **M10** was considered to be 1,2,3,4-tetrahydro-2-oxo-4-quinolinecarboxylic acid. **M23** had molecular ion $[M-H]^-$ at m/z 204.06679 and a characteristic fragment ion at m/z 158.06108, which were 14 Da (CH_2) higher than **M10**. Hence, **M23** was inferred as the methylation product of **M10**.

M26, **M32**, **M33** and **M35** had fragmentation ions at m/z 144.04553, 144.04550, 144.04536 and 144.04550, respectively, which were similar to the fragment behaviors of Gla A. They were tentatively identified as Gla A + H_2O+2H , Gla A- H_2O-2H , Gla A+ $2H$ and Gla A- H_2O for their fragment ions at m/z 303.14514, 221.08220, 243.12376 and 223.09743, which were 20 Da (H_2O+2H) higher, 2 Da ($2H$) higher, 20 Da ($-H_2O-2H$) lower and 18 Da ($-H_2O$) lower than the fragment ion at m/z 241.10838 of Gla A.

Analysis of metabolites of EA in intestinal bacteria

A total of 2 prototype component and metabolite were detected in intestinal bacteria. **M3** and **M20** was attributed to be EA (Ding et al., 2019). Obviously, hydrolyzation was the main metabolic pathway of EA in intestinal bacteria.

Analysis of metabolites of Gla A in intestinal bacteria

A total of 13 prototype components and metabolites were identified, including **M4**, **M6**, **M10**, **M14**, **M15**, **M18**, **M19**, **M21**, **M23**, **M28-M30** and **M34**. The result indicated that the possible metabolic pathways were dehydroxylation, hydroxylation, methylation, hydrolyzation, hydration and reduction.

M6 was detected with a characteristic ion at m/z 144.04547 and fragment ion at m/z 206.04602, which was 162 Da lower than **M4**.

It was suggested that **M6** was 1,2,3,4-tetrahydro-4-hydroxy-2-oxo-4-quinolinecarboxylic acid. **M21** was identified as a hydroxylation product of Gla A, for the fragment ion at m/z 359.13556, which was 16 Da (O) higher than the fragment ion at m/z 343.13876 of Gla A. **M34** was considered to be Gla A+CH₂, with [M-H]⁻ ion at m/z 606.21997 and characteristic ion at m/z 255.12416, which were 14 Da (CH₂) higher than Gla A. **M14**, **M19** and **M23** had fragmentation ions at m/z 146.04623, 146.04576 and 158.06108, respectively, which were similar with the fragment behaviors of Gla A. **M14**, **M19** and **M23** had molecular ion [M-H]⁻ at m/z 192.06677, 206.08246 and 204.06679, which were 2 Da (2H), 16 Da (CH₂+2H) and 14 Da (CH₂) higher than the fragment ion of **M10**. Therefore, **M14**, **M19** and **M23** were identified as 1,2,3,4-tetrahydro-2-oxo-4-quinolinecarboxylic acid+2H, 1,2,3,4-tetrahydro-2-oxo-4-quinolinecarboxylic acid+CH₂+2H and 1,2,3,4-tetrahydro-2-oxo-4-quinolinecarboxylic acid+CH₂, respectively.

4 Discussion

The PGS model was established in guinea pigs utilizing lithogenic diet and lincomycin. Lithogenic diet reduced the ability of gallbladder damage resistance, bile duct epithelial regeneration and liver synthesis of cholic acid. Additionally, the cholesterol from the lithogenic diet aggravated the burden on the liver. Lincomycin, on the other hand, caused gallbladder inflammation and stimulated mucus secretion to create an environment for the precipitation and accumulation of bile pigments. The UCB was supersaturated and contacted with Ca²⁺ in the bile, so the bilirubin calcium precipitation-dissolution lose balance to lead to the formation of stone bile (Gazali et al., 2021). Lincomycin with a lithogenic diet effectively decreased the molding time and increased the success rate.

The conjugated bilirubin in bile is hydrolyzed by endogenous glucuronidase to UCB and glucuronide, and then combined with calcium ions to precipitate bilirubin calcium. Typically, the level of UCB in total bilirubin was around 1% and improbable to form stone. When the content of UCB in bile increases, bilirubin calcium is produced, which becomes the basis of bile pigment stones (Dosch et al., 2019). DWPE significantly affected the biochemical changes of bile in guinea pigs. It may reverse the formation of biliary bile and prevent the formation of PGS by reducing the content of UCB and Ca²⁺ in bile. As can be conjectured from the histopathological, the effects of DWPE on gallstones guinea pigs might be related to the decrease of gallbladder cell damage and gallbladder mucosa abnormal proliferation.

We investigated the metabolism of DWPE and its main components EA and Gla A *in vitro*. DWPE, Gla A and EA were relatively stable in simulated gastric juice and intestinal juice. Thus, the composition changes in DWPE, Gla A and EA were indicated not influenced by the pH levels of gastric and intestinal juice, pepsin and trypsin. In addition, our laboratory found that DWPE, Gla A and EA were stable in liver S9 and intestinal S9. It is well known that intestinal bacteria play an important role in the metabolism of compounds (Sun et al., 2019). The stability study of DWPE, EA and Gla A in intestinal bacteria showed that both EA and Gla A in DWPE metabolized slowly compared with the monomer control, which was inferred that the complex components of the extract have a certain protective effect on EA and Gla A metabolism.

A total of 52 metabolites were identified *in vivo* in our earlier studies. The main metabolic reactions were dehydroxylation, methylation, hydrolysis, hydroxylation, sulfation and glucuronidation (Ren et al., 2022). A total of 35 metabolites were identified *in vitro*. Dehydroxylation, hydroxylation, hydrolysis, hydration, reduction and methylation were the main metabolic pathways of DWPE. Intestinal bacteria mainly mediated reduction and hydrolysis reactions, sulfation and glucuronidation metabolites of the prototype components were not detected. Compared with *in vivo* metabolism, the metabolites were reduced, except for some phase II metabolites, high relative content metabolites were also detected in intestinal bacteria metabolites. Therefore, the main chemical components in DWPE are mainly metabolized by intestinal bacteria. We speculated that DWPE was gradually transformed in intestinal bacteria, which were better absorbed in blood. In addition, previous studies in our laboratory reported that DWPE had a remodeling effect on intestinal bacteria (Ren et al., 2021). Thus it was inferred there was an interaction between the chemical components of DWPE and intestinal bacteria.

5 Conclusion

In this work, the therapeutic impact of DWPE on PGS was studied by assessing histopathological changes and bile biochemical indices. DWPE played a therapeutic role by regulating bile composition, promoting bile secretion, and reducing gallbladder cell damage and mucosa dysplasia. For additional investigation, UPLC-Q-Exactive Orbitrap MS was used to examine the metabolism of DWPE and its primary constituents EA and Gla A *in vitro*. Totally of 35 metabolites were detected. Hydrolyzation, methylation and reduction were the main metabolic pathway of DWPE in intestinal bacteria, which was the main metabolism organ. This study was helpful in understanding the pharmacodynamic substance of DWPE and provided a trustworthy new method for the treatment and fundamental investigation of PGS.

Conflict of interest

The authors declared no conflict of interest.

Author contributions

Xiao-qiu Liu and Shu-meng Ren designed the research; Shi-nuo Fang did the major experimental work and contributed in manuscript writing; Xia-jing Xu, Jing Ma and Qing-zhu Zhang participated in part of the experiments; Ying-ni Pan and Dong-mei Wang revised the paper.

Acknowledgements

This study was supported by National Natural Science Foundation of China (No. 82204609).

References

- Ashraf, S., Arfeen, A., Amjad, S., & Ahmed, Z. (2021). Effect of walnut (*Juglans Regia*) consumption on hyperlipidemic adults. *Food Science and Technology*, 41(Suppl. 2), 432-438. <http://dx.doi.org/10.1590/fst.29720>.
- Beckingham, I. J. (2020). Gallstones. *Surgery*, 38(8), 453-462. <http://dx.doi.org/10.1016/j.mpsur.2020.06.002>.

- Bidanchi, R. M., Lalrindika, L., Khushboo, M., Bhanushree, B., Dinata, R., Das, M., Nisa, M., Lalrinzuali, S., Manikandan, B., Saeed-Ahmed, L., Sanjeev, S., Murthy, Roy, V. K., & Gurusubramanian, G. (2022). Antioxidative, anti-inflammatory and anti-apoptotic action of ellagic acid against lead acetate induced testicular and hepato-renal oxidative damages and pathophysiological changes in male Long Evans rats. *Environmental Pollution*, 302, 119048. <http://dx.doi.org/10.1016/j.envpol.2022.119048>. PMID:35219795.
- Chen, Q., Deng, X., Qiang, L., Yao, M., Guan, L., Xie, N., Zhao, D., Ma, J., Ma, L., Wu, Y., & Yan, X. (2021). Investigating the effects of walnut ointment on non-healing burn wounds. *Burns*, 47(2), 455-465. <http://dx.doi.org/10.1016/j.burns.2020.06.032>. PMID:32736884.
- Cheng, Q., Zhang, Y., Lin, Q., Tian, Y., & Bao, Y. (2022). Study on the antioxidant activity of β -sitosterol and stigmaterol from Sacha Inchi oil and Prinsepia oil added to walnut oil. *Food Science and Technology*, 42, e69522. <http://dx.doi.org/10.1590/fst.69522>.
- Chinese Pharmacopoeia Commission. (2020). *Chinese pharmacopoeia*. Beijing: China Medical Science and Technology Press.
- Dhungana, N., Morris, C., & Krasowski, M. D. (2017). Operational impact of using a vanadate oxidase method for direct bilirubin measurements at an academic medical center clinical laboratory. *Practical Laboratory Medicine*, 8, 77-85. <http://dx.doi.org/10.1016/j.plabm.2017.05.004>. PMID:28856232.
- Ding, C., Liu, Q., Li, P., Pei, Y., Tao, T., Wang, Y., Yan, W., Yang, G., & Shao, X. (2019). Distribution and quantitative analysis of phenolic compounds in fractions of Japonica and Indica rice. *Food Chemistry*, 274, 384-391. <http://dx.doi.org/10.1016/j.foodchem.2018.09.011>. PMID:30372955.
- Dosch, A. R., Imagawa, D. K., & Jutric, Z. (2019). Bile metabolism and lithogenesis: an update. *The Surgical Clinics of North America*, 99(2), 215-229. <http://dx.doi.org/10.1016/j.suc.2018.12.003>. PMID:30846031.
- Duan, J., Li, Y., Gao, H., Yang, D., He, X., Fang, Y., & Zhou, G. (2020). Phenolic compound ellagic acid inhibits mitochondrial respiration and tumor growth in lung cancer. *Food & Function*, 11(7), 6332-6339. <http://dx.doi.org/10.1039/D0FO01177K>. PMID:32608435.
- Gao, P., Liu, R., Jin, Q., & Wang, X. (2022). Key chemical composition of walnut (*Juglans regia*, L.) oils generated with different processing methods and their cholesterol-lowering effects in HepG2 cells. *Food Bioscience*, 45, 101436. <http://dx.doi.org/10.1016/j.fbio.2021.101436>.
- Gazali, Z., Kumar, R., Rai, P. K., Rai, P. K., Rai, A. K., & Thakur, S. N. (2021). Discrimination of gallbladder stone employing Laser-Induced Breakdown Spectroscopy (LIBS) and Photoacoustic Spectroscopy (PAS). *Spectrochimica Acta. Part A: Molecular and Biomolecular Spectroscopy*, 260, 119948. <http://dx.doi.org/10.1016/j.saa.2021.119948>. PMID:34030035.
- Haramiishi, R., Okuyama, S., Yoshimura, M., Nakajima, M., Furukawa, Y., Ito, H., & Amakura, Y. (2020). Identification of the characteristic components in walnut and anti-inflammatory effect of gallsreginin A as an indicator for quality evaluation. *Bioscience, Biotechnology, and Biochemistry*, 84(1), 187-197. <http://dx.doi.org/10.1080/09168451.2019.1670046>. PMID:31566092.
- Lu, Q., Jiang, Z., Wang, Q., Hu, H., & Zhao, G. (2021). The effect of Tauroursodeoxycholic acid (TUDCA) and gut microbiota on murine gallbladder stone formation. *Annals of Hepatology*, 23, 100289. <http://dx.doi.org/10.1016/j.aohep.2020.100289>. PMID:33217585.
- Qu, W., Fan, W., Feng, Y., Li, Y., Ma, H., & Pan, Z. (2021). Preparation of heat-sensitivity proteins from walnut meal by sweep frequency ultrasound-assisted alkali extraction. *Journal of Food Quality*, 2021, 1-12. <http://dx.doi.org/10.1155/2021/9478133>.
- Ren, S. M., Zhang, Q. Z., Chen, M. L., Jiang, M., Zhou, Y., Xu, X. J., Wang, D. M., Pan, Y. N., & Liu, X. Q. (2021). Anti-NAFLD effect of defatted walnut powder extract in high fat diet-induced C57BL/6 mice by modulating the gut microbiota. *Journal of Ethnopharmacology*, 270, 113814. <http://dx.doi.org/10.1016/j.jep.2021.113814>. PMID:33444725.
- Ren, S. M., Zhang, Q. Z., Jiang, M., Chen, M. L., Xu, X. J., Wang, D. M., Pan, Y. N., & Liu, X. Q. (2022). Systematic characterization of the metabolites of defatted walnut powder extract in vivo and screening of the mechanisms against NAFLD by UPLC-Q-Exactive Orbitrap MS combined with network pharmacology. *Journal of Ethnopharmacology*, 285, 114870. <http://dx.doi.org/10.1016/j.jep.2021.114870>. PMID:34848359.
- Ren, S., Yan, X., Ma, J., Pan, Y., Zhang, W., Wang, D., Fei, Z., & Liu, X. (2018). Defatted walnut powder extract reduces cholesterol gallstones formation in C57BL/6 mice by downregulating the levels of ABCG5/8 in the liver and NPC1L1 in the intestine. *Journal of Functional Foods*, 48, 85-91. <http://dx.doi.org/10.1016/j.jff.2018.06.017>.
- Ruiz-Caro, P., Espada-Bellido, E., Garcia-Guzman, J. J., Bellido-Milla, D., Vazquez-Gonzalez, M., Cubillana-Aguilera, L., & Palacios-Santander, J. M. (2022). An electrochemical alternative for evaluating the antioxidant capacity in walnut kernel extracts. *Food Chemistry*, 393, 133417. <http://dx.doi.org/10.1016/j.foodchem.2022.133417>. PMID:35691065.
- Sun, C., Chen, L., & Shen, Z. (2019). Mechanisms of gastrointestinal microflora on drug metabolism in clinical practice. *Saudi Pharmaceutical Journal*, 27(8), 1146-1156. <http://dx.doi.org/10.1016/j.jsps.2019.09.011>.
- Swarne, E., Srikanth, M. S., Shreyas, A., Desai, S., Mehdi, S., Gangadharappa, H. V., & Krishna, K. L. (2021). Recent advances, novel targets and treatments for cholelithiasis; a narrative review. *European Journal of Pharmacology*, 908, 174376. <http://dx.doi.org/10.1016/j.ejphar.2021.174376>. PMID:34303667.
- Tošović, J., & Bren, U. (2020). Antioxidative action of ellagic acid-A kinetic DFT study. *Antioxidants*, 9(7), 587. <http://dx.doi.org/10.3390/antiox9070587>. PMID:32640518.
- Wang, D. Q. H., Portincasa, P., & Wang, H. H. (2020). Bile formation and pathophysiology of gallstones. In E. J. Kuipers (Ed.), *Encyclopedia of gastroenterology* (2nd ed., pp. 287-306). Amsterdam: Academic Press. <http://dx.doi.org/10.1016/B978-0-12-801238-3.65861-0>.
- Wang, X., Li, X., Wang, R., Wang, L., Fan, S., Wang, X., Xu, X., Yan, X., He, T., Ren, X., & She, G. (2019). Human gastrointestinal metabolism of the anti-rheumatic fraction of Dianbaizhu (*Gaultheria leucocarpa* var. *yunnanensis*) in vitro: elucidation of the metabolic analysis in gastric juice, intestinal juice and human intestinal bacteria by UPLC-LTQ-Orbitrap-MS(n) and HPLC-DAD. *Journal of Pharmaceutical and Biomedical Analysis*, 175, 112791. <http://dx.doi.org/10.1016/j.jpba.2019.112791>. PMID:31398629.
- Wei, Z., Chen, J., Zuo, F., Guo, J., Sun, X., Liu, D., & Liu, C. (2023). Traditional Chinese medicine has great potential as candidate drugs for lung cancer: a review. *Journal of Ethnopharmacology*, 300, 115748. <http://dx.doi.org/10.1016/j.jep.2022.115748>. PMID:36162545.
- Xu, X., Ren, S., Wang, D., Ma, J., Yan, X., Guo, Y., Liu, X., & Pan, Y. (2022a). Optimization of extraction of defatted walnut powder by ultrasonic assisted and artificial neural network. *Food Science and Technology*, 42, e53320. <http://dx.doi.org/10.1590/fst.53320>.
- Xu, X., Song, Y., Jiang, M., Liu, M., Zhang, X., Wang, D., Pan, Y., Ren, S., & Liu, X. (2022b). An assessment of the potential of defatted walnut powder extract against hyperlipidemia-intensified L-arginine-induced acute pancreatitis. *Food Science and Technology*, 42, e19722. <http://dx.doi.org/10.1590/fst.19722>.
- Yao, C., Wu, S., Liu, Z., & Li, P. (2019). A deep learning model for predicting chemical composition of gallstones with big data in medical Internet of Things. *Future Generation Computer Systems*, 94, 140-147. <http://dx.doi.org/10.1016/j.future.2018.11.011>.

Supplementary Material

Supplementary material accompanies this paper.

Table S1. Detailed mass spectral data of DWPE in intestinal bacteria.

This material is available as part of the online article from <https://doi.org/10.1590/fst.115222>